ISBN: 978-3-95450-215-8 ISSN: 2226-0366 doi:10.18429/JACoW-LINAC2022-MOPOGE13

ACCELERATION EFFICIENCY OF TE-MODE STRUCTURES FOR PROTON LINACS

J. Tamura*, Y. Kondo, T. Morishita, JAEA/J-PARC, Ibaraki, Japan
F. Naito, M. Otani, KEK/J-PARC, Ibaraki, Japan

Abstract

High-energy proton linacs generally consist of various types of cavity structures because the acceleration efficiency of a cavity depends on the velocity of the beam particle. Alvarez drift-tube linacs (DTLs) and transverse-electric (TE)-mode accelerating structures such as interdigital H-mode (IH) DTL and crossbar H-mode (CH) DTL are widely used in the low-energy section of the proton linacs. In this study, shunt impedances of these cavity structures, including higher-order TE_{31} and TE_{41} DTLs, are simulated by applying a very simple structural configuration. This study shows that TE_{m1} DTLs with smaller angular index m have higher shunt impedances whereas the axisymmetry of the electric field improves as m increases, and that the shunt impedances of TE_{11} and TE_{21} DTLs are higher than those of Alvarez DTLs especially in the low energy region immediately after a radiofrequency quadrupole (RFQ).

INTRODUCTION

Various types of cavity structures are generally used in high-energy proton linacs. This is, particularly in normal-conducting structures, because cavity's acceleration efficiency varies with the velocity of the beam particle. For low-energy proton beam acceleration, while Alvarez DTLs are the most prevalent, TE-mode structures, which could also be called H-mode structures, are also widely used. At present, the typical TE-mode accelerating structures are IH-DTL and CH-DTL [1–3], which are based on TE_{11}-mode and TE_{21}-mode pillbox cavities, respectively. Because the optimal cavity structure for proton linacs may be a subject of frequent argument [4], we investigated the acceleration efficiency of Alavarez DTLs and TE-mode accelerating structures including higher-order TE_{31} and TE_{41} DTLs. In this study, the shunt impedances of these cavity structures for proton energies of 2-100 MeV were simulated by using the CST Studio Suite.

SIMULATION MODEL

In this simulation study, 162 MHz TE-mode DTLs and 324 MHz Alvarez DTLs were examined by applying the following very simple structural configuration. Each cavity has four drift tubes (DTs) supported by stems and two end-cell half-DTs attached to the entry and exit lids, respectively. Therefore, Each cavity has five acceleratring gaps. The stems were all rod-shaped with a fixed diameter of 20 mm for simplicity. The cell length, which is defined by the distance between adjacent gap centers, changes with the beam velocity as $\beta\lambda/2$ for TE-mode DTLs and as $\beta\lambda$ for Alvarez DTLs, where β is the beam velocity relative to the speed of light and λ is the wavelength. For a given proton energy, the cell length of 162 MHz TE-mode DTLs is always the same as that of 324 MHz Alvarez DTLs.[1] Giving a priority to the structural simplicity, all cell lengths within a cavity were kept the same. Figure 1 shows the applied DT geometry. Wheareas the ratio of gap length (g) to cell length was set to $g/(\beta\lambda/2) = 0.50$ for TE-mode DTLs, two ratios of $g/\beta\lambda = 0.50$ and 0.25 were applied for Alvarez DTLs. Figures 2-6 show examples of the simulation models for TE_{m1} DTLs ($m = 1, 2, 3, 4$) and Alvarez DTL ($g/\beta\lambda = 0.50$), which cell lengths and cavity diameters are adjusted for a 10 MeV proton beam. Each electric field distribution of the corresponding pillbox cavity is shown on the left side.

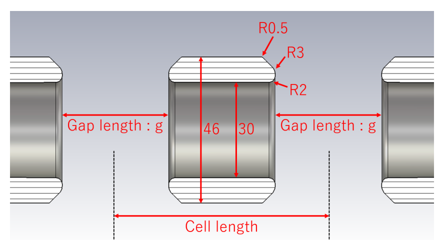

Figure 1: DT geometry applied to the simulation.

FIGURES OF MERIT

In each simulation model, only the cavity's transverse diameter was adjusted so that the resonant frequency becomes 162 MHz and 324 MHz for TE-mode DTLs and Alvarez DTLs, respectively. Obtained cavity diameters are shown in Fig. 7. The TE_{m1}-mode DTL has a smaller transverse diameter with smaller angular index m.

The longitudinal electric field distribution along the beam axis is essential for evaluating the cavity's acceleration efficiency. Figure 8 shows the obtained field distribution for the cavities accelerating a 10 MeV proton beam. In this figure, each field amplitude is normalized so that the stored energy is 1 Joule. Whereas the flat field distributions are produced in the Alvarez DTLs, the electric fields of the TE-mode DTLs decrease toward the end of the cavity because the TE field cannot exist paralled to the end walls of a conducting cavity. As shown in Fig. 8, the TE_{m1} DTL with smaller m provides higher gap voltage with respect to the unit stored energy, in other words, the so-called r/Q is larger in the lower-order

[1] For example, the cell lengths corresponding to the proton energies of 2, 10, 20, and 100 MeV are 60.3, 134.0, 188.1, and 396.2 mm with β's of 0.065, 0.145, 0.203, and 0.428, respectively.

* jtamura@post.j-parc.jp

ISBN: 978-3-95450-215-8 ISSN: 2226-0366 doi:10.18429/JACoW-LINAC2022-MOPOGE13

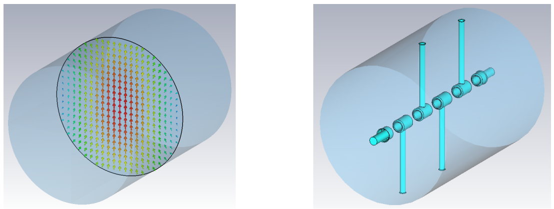

Figure 2: [left] Electric field of TE_{11}-mode pillbox cavity. [right] Simulation model of TE_{11} DTL (IH-DTL).

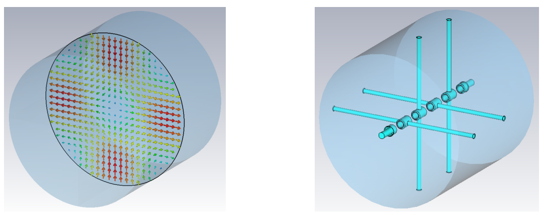

Figure 3: [left] Electric field of TE_{21}-mode pillbox cavity. [right] Simulation model of TE_{21} DTL (CH-DTL).

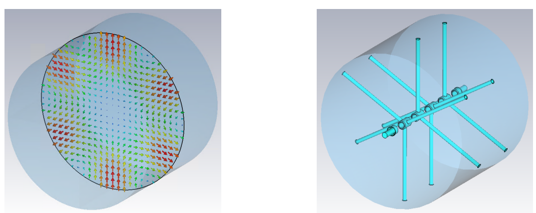

Figure 4: [left] Electric field of TE_{31}-mode pillbox cavity. [right] Simulation model of TE_{31} DTL.

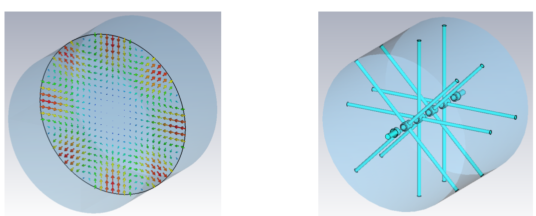

Figure 5: [left] Electric field of TE_{41}-mode pillbox cavity. [right] Simulation model of TE_{41} DTL.

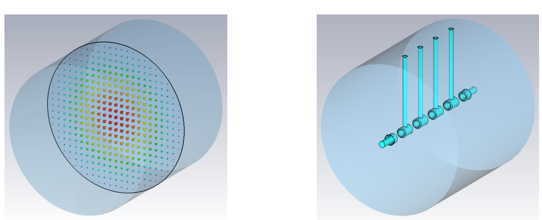

Figure 6: [left] Electric field of TM_{010}-mode pillbox cavity. [right] Simulation model of Alvarez DTL.

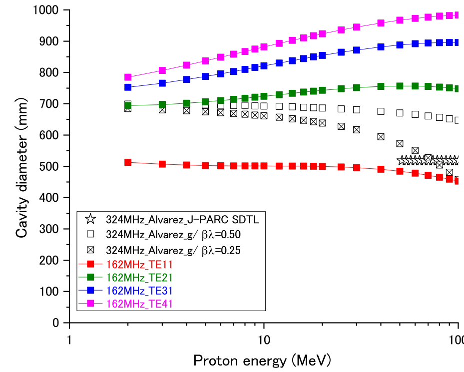

Figure 7: Cavity diameters.

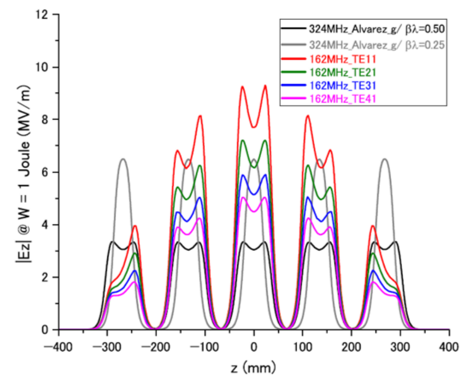

Figure 8: Longitudinal (absolute) electric field distribution along the beam axis of the simulated cavities accelerating a 10 MeV proton beam.

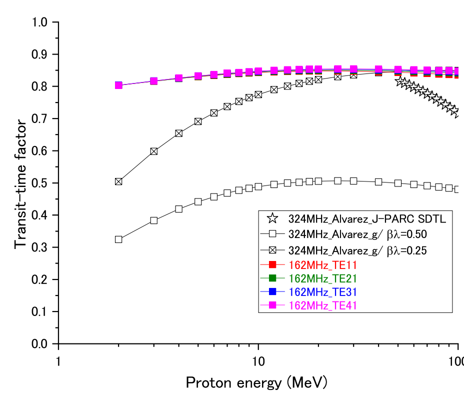

Figure 9: Transit-time factors.

TE_{m1} DTLs. Furthermore, it can be seen that the TE-mode DTLs have higher axial voltage than Alvarez DTLs in this low energy accelerating section. Figure 9 shows the transit-time factors (TTFs) calculated from the longitudinal field distribution. The TTFs of the Alvarez DTLs decrese at the low energy side due to the entry of an electric field inside DTs. Because the TE-mode DTLs have a gap-to-gap phase difference of π radians whereas the Alvarez DTLs have zero, the TTFs of TE-mode DTLs can be as high as 0.8 or more, even with such a large gap length relative to cell length.

The cavity's acceleration efficiency is assessed in terms of power efficiency. Figure 10 shows the simulated Q_0 values obtained by setting the copper conductivity of $\sigma = 5.8 \times 10^7$ S/m. The Q_0 values of the TE-mode DTLs are less sensitive to the cell length and are much smaller than those

ISBN: 978-3-95450-215-8 ISSN: 2226-0366 doi:10.18429/JACoW-LINAC2022-MOPOGE13

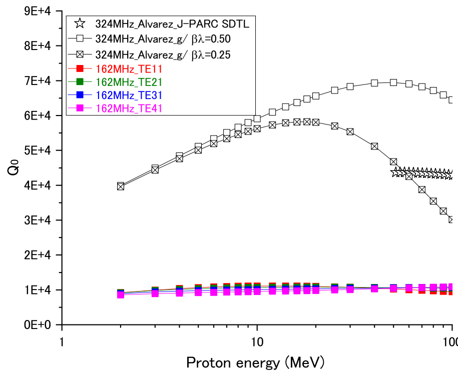

Figure 10: Unloaded Q values.

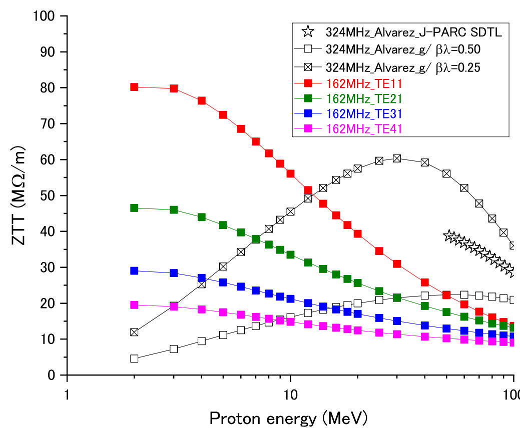

Figure 11: Effective shunt impedances per unit length.

of Alvarez DTLs. Figure 11 shows the obtained effective shunt impedances per unit length. The TE_{m1} DTLs with smaller m have higher shunt impedances. In the low energy accelerating region such as immediately after an RFQ, the shunt impedances of TE-mode DTLs, especially TE_{11} and TE_{21} DTLs, are higher than those of Alvarez DTLs. These are contributed by the higher r/Q of lower-order TE_{m1} DTLs. Table 1 shows the simulated RF losses distribution. It is clear that most of the RF losses in the TE-mode DTLs occur at the stems, unlike in the Alvarez cavity.

Table 1: RF Losses distribution in %. These cavities are for accelerating a 10 MeV proton beam.

Cavity	P_{Tank}	P_{Lids}	P_{Stems}	P_{DTs}
Alvarez ($g/\beta\lambda = 0.50$)	59.9	32.5	6.2	1.4
Alvarez ($g/\beta\lambda = 0.25$)	54.0	31.2	7.1	7.7
TE_{11}	18.3	2.0	76.1	3.6
TE_{21}	14.7	1.4	83.5	0.5
TE_{31}	13.3	0.9	85.7	0.2
TE_{41}	12.1	0.6	87.2	0.1

The axisymmetric property of the electric field was evaluated for the TE-mode DTLs. As is generally known, a dipole electric field remains in an IH-DTL, and the beam is deflected by the dipole field with reversed polarity each time it passes through the gap. Similarly, TE_{21}, TE_{31}, and TE_{41} DTLs generate quadrupole, sextupole, and octapole electric field, respectively. Figure 12 shows the ratios of multi-pole field amplitude to longitudinal field strength. Except for

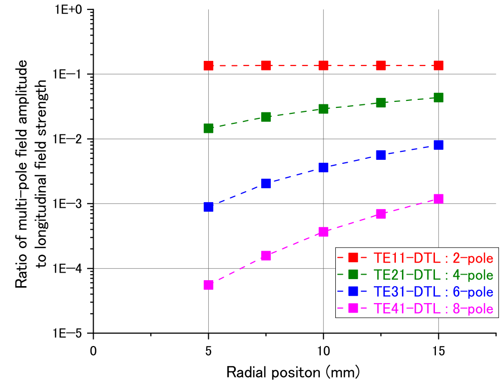

Figure 12: Multi-pole field amplitude relative to the longitudinal field strength for TE-mode DTLs accelerating a 10 MeV proton beam.

TE_{11} DTL, the multi-pole field decreases toward the cavity's radial center. For the TE_{m1} DTLs, the axial symmetry of the electric field improves as m increases.

SUMMARY

This simulation study shows that TE_{m1} DTLs with smaller m have higher shunt impedances, and especially in the low energy accelerating region like immediately after an RFQ, the lower-order TE_{m1} DTLs have have larger shunt impedances than Alvarez DTLs. Concering the axial symmetric property of the generated electric field, less multi-pole field remains in higher order TE_{m1} DTLs. It should be added here that the choices of cavity structure should be considered not only in terms of acceleration efficiency, but also in terms of practical cavity size, efficient cavity cooling, transverse beam convergence elements, surface peak electric field, etc.

ACKNOWLEDGMENTS

We would like to thank the members of MYRRHA Accelerator Design and Test team for their continued interest and encouragement in this study.

REFERENCES

[1] Thomas P. Wangler, *RF Linear Accelerators*, New York, NY, USA: Wiley, 2008.

[2] F. Gerigk, "Cavity types", CERN Accelerator School: RF for Accelerators, CERN-2011-007, pp. 277–298.

[3] MYRRHA Accelerator Design and Test team, "MINERVA 100-MeV Accelerator Technical Design Report", SCK-CEN, Mol, Belgium.

[4] C. Plostinar, "Comparative Assessment of HIPPI Normal Conducting Structures", CARE-Report-2008-071-HIPPI.